# Mask R-CNN based coronary artery segmentation in coronary computed tomography angiography

Fu, Yabo, Guo, Bangjun, Lei, Yang, Wang, Tonghe, Liu, Tian, et al.

Yabo Fu, Bangjun Guo, Yang Lei, Tonghe Wang, Tian Liu, Walter Curran, Longjiang Zhang, Xiaofeng Yang, "Mask R-CNN based coronary artery segmentation in coronary computed tomography angiography," Proc. SPIE 11314, Medical Imaging 2020: Computer-Aided Diagnosis, 113144F (16 March 2020); doi: 10.1117/12.2550588

SPIE.

Event: SPIE Medical Imaging, 2020, Houston, Texas, United States

# Mask R-CNN based Coronary Artery Segmentation in Coronary Computed Tomography Angiography

Yabo Fu[a], Bangjun Guo[a, b, c], Yang Lei[a], Tonghe Wang[a], Tian Liu[a], Walter Curran[a], Longjiang Zhang[b, c] and Xiaofeng Yang[a*]

[a]Department of Radiation Oncology and Winship Cancer Institute, Emory University, Atlanta, GA 30322
[b]Department of Medical Imaging, Jinling Hospital, Southern Medical University, Nanjing, China, 210002
[c]Department of Medical Imaging, Jinling Hospital, Medical School of Nanjing University, Nanjing, China, 210002
*Corresponding to: xiaofeng.yang@emory.edu

## ABSTRACT

Automated segmentation of the coronary artery in coronary computed tomographic angiography (CCTA) is important for clinicians in evaluating patients with coronary artery disease. Tradition visual interpretation of coronary artery stenosis exist inter-observer variability and time-consuming. The purpose of this work is to develop a deep learning-based framework for coronary artery segmentation on CCTA. We propose to use Mask R-CNN for the coronary artery segmentation. To avoid the interferences from pulmonary vessels, we propose to mask out the lung region prior to Mask R-CNN training. The network was trained using 20 patients' CCTA datasets and tested using another 5 patients' CCTA datasets. The mean of the Dice similarity coefficient (DSC) were 0.90±0.01 respectively, which demonstrated the segmentation accuracy of the proposed method.

**Keywords:** coronary artery, segmentation, CTA, deep learning

## 1. INTRODUCTION

Cardiovascular diseases are the leading cause of disability and death worldwide [1]. Coronary artery disease (CAD) is primarily caused by coronary artery narrowing due to atherosclerosis [2]. Nowadays, coronary computed tomographic angiography (CCTA) plays a crucial role in detecting coronary artery disease (CAD) and is regarded as an effective means of ruling out CAD [3]. Moreover, tradition visual interpretation of coronary artery stenosis exists inter-observer variability and time-consuming [4]. Therefore, automated segment the coronary artery is important for the clinicians in evaluating patients with CAD.

Previously studies have reported using different image processing approaches, such as graph-cut [5], level-set [6] to segment coronary artery [7, 8]. Coronary artery centerlines were typically extracted to support artery reconstruction in stenosis and plaque detection. Lesage *et al.* provided a review on centerline extraction methods, dividing them in to three main categories [9]. Many methods are based on shortest path computation given two end points on the artery with various vesselness measurements in the path cost such as Hessian vesselness [10]. Zhou *et al.* employed a multiscale filtering and dynamic balloon tracking method to extract coronary artery tree [11]. Kerkeni *et al.* segmented 2D X-ray angiograms using a multiscale region growing method which considers both vesselness and direction [12]. Similarly, Tian *et al.* also used a region growing method to automatically segment coronary arteries. They first segmented the heart region using a multi-atlas-based method. Then, the vessel structures within the heart were enhanced using a 3D multiscale line filter prior to the region growing [13]. Yang *et al.* proposed to use an improved Frangi's vesselness filter in coronal artery centerline extraction [14].

Medical Imaging 2020: Computer-Aided Diagnosis, edited by Horst K. Hahn, Maciej A. Mazurowski, Proc. of SPIE Vol. 11314, 113144F · © 2020 SPIE
CCC code: 1605-7422/20/$21 · doi: 10.1117/12.2550588

Handcrafted vesselness measurements are not optimal in the image context. Therefore, machine learning-based vesselness was proposed by learning from expert-annotated datasets. Zheng *et al.* trained a classifier which assigns high score to artery voxels and a low score to outside voxels by using a probabilistic boosting tree [15]. Recently, deep learning-based methods have changed the landscape of image segmentation tasks and outperformed many traditional image segmentation [16-31]. Huang *et al.* employed 3D U-Net for coronary artery segmentation on CCTA with and without vessel centerline. They concluded that the network performed better with centerline and achieved a Dice of 0.82 [32]. Wolterink *et al.* proposed to use a 3D dilated CNN to predict the most likely directions and radius of an artery at a given point in CCTA image [33]. Their network was trained on 8 CCTA images with 32 manually annotated centerlines. The datasets used is from the MICCAI 2008 coronary artery tracking challenge. They have concluded that the neural network can determine the direction and radius of the coronary lumen with high speed and accuracy. Later, the same group proposed a graph convolutional networks (GCN) for coronary artery segmentation [34]. Instead of directly predicting the artery masks, they used the GCN to predict the vertices spatial location of artery lumen surface mesh.

In this paper, we propose to use Mask R-CNN [35-37] for the coronary artery segmentation. To avoid the interferences from pulmonary vessels, we propose to mask out the lung region prior to Mask R-CNN training. The network was trained using 20 patients' CCTA datasets and tested using another 5 patients' CCTA datasets. The mean of the Dice similarity coefficient (DSC) were 0.90±0.01 respectively, which demonstrated the segmentation accuracy of the proposed method.

## 2. MATERIAL AND METHODS

### 2.1 Segmentation using Mask R-CNN

Fig.1. shows the coronary artery segmentation framework which includes pre-processing, Mask R-CNN and post-processing. In pre-processing, pulmonary vessels that share similar structures with the coronary arteries were removed by masking out the lung region. We first segmented the lung volume using intensity thresholding and morphological operations. The lung mask was then used to erase the pulmonary vessel information prior to Mask R-CNN training. We chose to use Mask R-CNN because it is suitable to segment the coronary artery since the coronary arteries appear to be multiple small tubular structures in the axial CCTA images. Compared to the large heart volume, the small artery structure often introduces significant class imbalance problems, which impairs the performance of whole volume-based 3D CNN. Whole volume 3D training is not necessarily efficient in modelling the tiny artery features given the large amount of memory required. Additionally, whole volume 3D training needs a large set of training datasets which are often not available. Therefore, we propose to train the Mask R-CNN on axial 2D images.

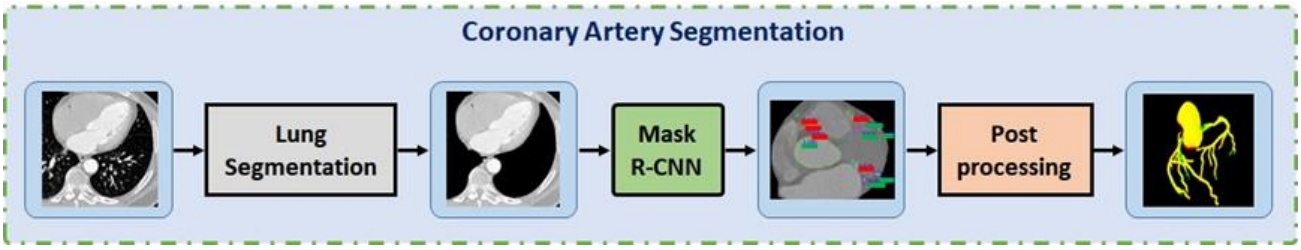


**Figure 1.** Schematic flow-chart of the proposed framework for coronary artery segmentation. The framework includes pre-processing, Mask R-CNN and post-processing.

In Mask R-CNN, a region proposal network [5, 7] was utilized to detect many potential regions of interest (ROIs) prior to segmentation. ROI-Alignment that directly extract patched features from the backbone-generated feature maps was used to deal with inconsistent ROI sizes. Class imbalance problem was mitigated by performing the segmentation within each ROI. To overcome the shortage of training datasets, the region proposal network was trained using transfer learning. Trained Resnet-50 network parameters were used to initialize the training parameters of the region proposal network. Additionally, data augmentations were used to enlarge the variety of the training data. Regional proposal anchors of sizes [8, 16, 32, 64 128] were used to cover the sizes of potential ROI candidates. Anchor ratios of [0.5 1 2]

were used to account for different potential ROI shapes. In the inference stage, the trained network predicted the coronary artery labels with a confidence value, indicating the likelihood of the mask being true positive.

In post-processing, we used a threshold value of 0.6 on the confidence values of each predicted masks to generate the initial coronary artery masks. The relatively small threshold value of 0.6 was based on our observation that smaller arteries that were not labelled in the ground truth datasets were often predicted with lower confidence value. The relatively low confidence value does not necessarily indicate it is a false positive. Finally, a morphological close operation was performed using sphere element structure to ensure that the segmented arteries were connected as a single vasculature structure. Small isolated islands were considered as noise and removed to generate the final mask.

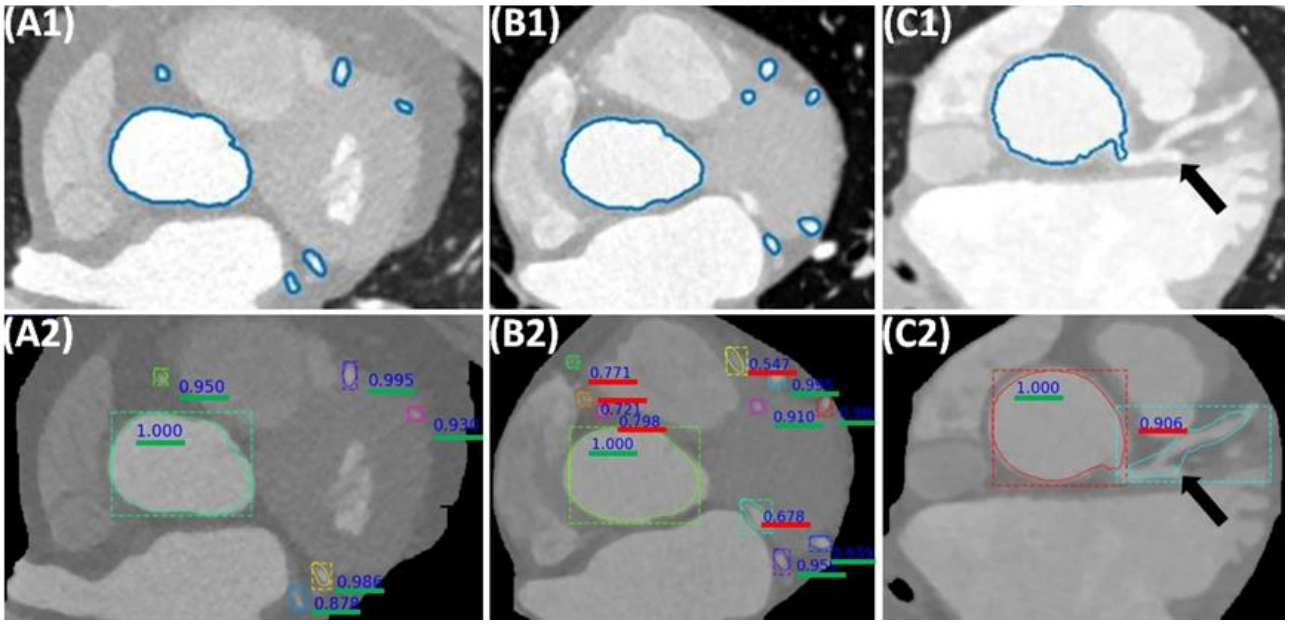


**Figure 2.** Manual contour (A1, B1, C1) and the ROI proposals (A2, B2, C2). Positive ROI proposals were marked using green underscore lines. 'Negative' ROI proposals were marked using red underscore lines. (A2) shows all positive ROI proposals that correspond to the ground truth in (A1). (B2) includes five 'negative' ROI proposals and six positive ROI proposals. (C2) shows one 'negative' proposal which was positive proposal, which is caused by inaccurate manual delineations highlighted using the black arrow.

## 3. RESULTS

To test the proposed method, we applied it to 20 patients' CCTA (0.28×0.28×0.50 mm3). Manual coronary artery contours were used as the ground truth. Fig. 2 shows examples of the comparison between the proposed ROIs and the ground truth. Positive ROI proposals were marked using green underscore lines. 'Negative' ROI proposals were marked using red underscore lines. Fig.2-(A2) shows all positive ROI proposals that correspond to the ground truth in Fig.2-(A1). Fig.2-(B2) includes five 'negative' ROI proposals and six positive ROI proposals. The five 'negative' ROI proposal are not necessarily all true negatives. For example, the three proposals with confidence values of 0.77, 0.72 and 0.79 in Fig.2-(B2) were arteries that were finer than the ground truth. Fig.2-(C2) shows one false 'negative' proposal, which is caused by inaccurate ground truth delineations highlighted using the black arrow. Fig.3. shows 3D rendering of the comparison between ground truth and the automatic segmentation results. Ground truth was shown in red color, the automatic segmentation results were shown in green color, and the overlap between the ground truth and automatic segmentation results were shown in yellow color. To quantitatively evaluate the segmentation performance of the proposed method, we calculated the Dice similarity coefficient (DSC) [38], between the ground truth and segmentation. Results were shown in Table 1.

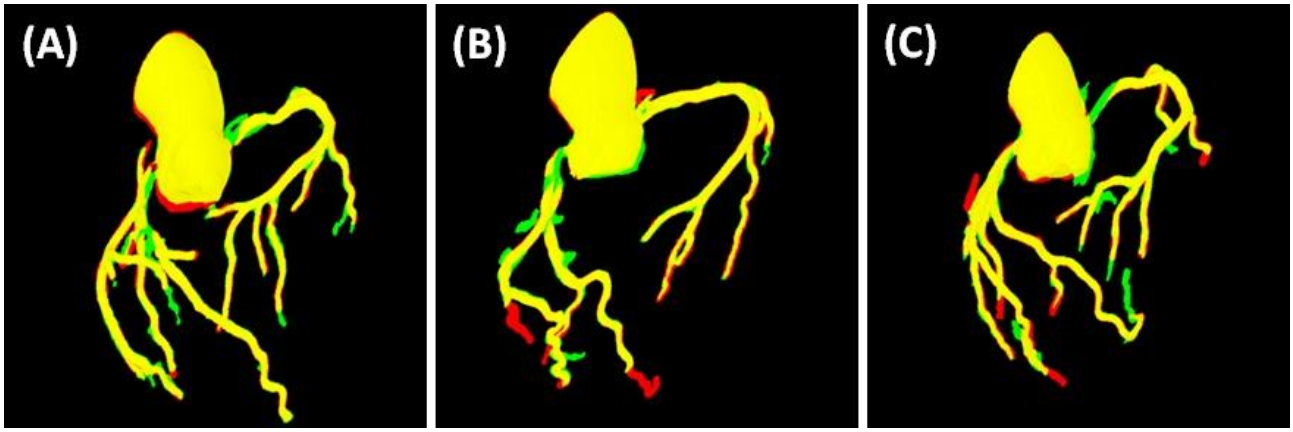


**Figure 3.** 3D rendering of coronary artery of three patients. Ground truth was shown in red color, the automatic segmentation results were shown in green color, and the overlap between the ground truth and automatic segmentation results were shown in yellow color.

**Table 1.** Dice scores of the proposed method.

| Mean ± Std | Mean | Std |
|---|---|---|
| Proposed | 0.90 | 0.01 |

## 4. DISCUSSION AND CONCLUSION

CCTA images plays an important role in the diagnosis of anatomical or functional severity of coronary artery stenosis [39]. Coronary artery segmentation can facilitate personalized coronary lumen surface meshing which is required in stenosis detection [7] and blood flow simulation [40]. However, manual annotation of the full coronary artery tree is time-consuming, tedious and slow. Therefore, automatic methods are required to segment the coronary artery. It is challenging to segment coronary artery on CCTA images due to their small volumes, complex shapes and image noise. The coronary junction often presents additional challenges to the segmentation. For deep learning-based methods, coronary arteries are small tubular structures inside the heart which causes significant class imbalance problem during network training. Therefore, the coronary arteries are usually misclassified as the background, leading to truncated artery segmentation.

In this study, we propose to use Mask R-CNN to segment coronary artery. This approach could mitigate the class imbalance problem by detecting artery ROIs prior to coronary arteries segmentation. To summarize, we have investigated a novel deep learning-based approach to segment the coronary artery from CCTA and demonstrated its reliability. Experimental validation has been performed to demonstrate it clinical feasibility and accuracy. This segmentation technique could be a useful tool for clinicians in evaluating patients with CAD.

## REFERENCES

[1] N. J. Pagidipati, and T. A. Gaziano, “Estimating deaths from cardiovascular disease: a review of global methodologies of mortality measurement,” Circulation, 127(6), 749-56 (2013).

[2] G. W. Stone, A. Maehara, A. J. Lansky *et al.*, “A Prospective Natural-History Study of Coronary Atherosclerosis,” New England Journal of Medicine, 364(3), 226-235 (2011).

[3] A. Coenen, M. M. Lubbers, A. Kurata *et al.*, “Fractional flow reserve computed from noninvasive CT angiography data: diagnostic performance of an on-site clinician-operated computational fluid dynamics algorithm,” Radiology, 274(3), 674-83 (2015).
[4] W. B. Meijboom, M. F. Meijs, J. D. Schuijf *et al.*, “Diagnostic accuracy of 64-slice computed tomography coronary angiography: a prospective, multicenter, multivendor study,” J Am Coll Cardiol, 52(25), 2135-44 (2008).
[5] M. Schaap, L. Neefjes, C. Metz *et al.*, “Coronary lumen segmentation using graph cuts and robust kernel regression,” Inf Process Med Imaging, 21, 528-39 (2009).
[6] J. Brieva, E. Gonzalez, F. Gonzalez *et al.*, “A level set method for vessel segmentation in coronary angiography,” Conf Proc IEEE Eng Med Biol Soc, 6, 6348-51 (2005).
[7] H. A. Kirisli, M. Schaap, C. T. Metz *et al.*, “Standardized evaluation framework for evaluating coronary artery stenosis detection, stenosis quantification and lumen segmentation algorithms in computed tomography angiography,” Med Image Anal, 17(8), 859-76 (2013).
[8] R. Shahzad, H. Kirisli, C. Metz *et al.*, “Automatic segmentation, detection and quantification of coronary artery stenoses on CTA,” Int J Cardiovasc Imaging, 29(8), 1847-59 (2013).
[9] D. Lesage, E. D. Angelini, I. Bloch *et al.*, “A review of 3D vessel lumen segmentation techniques: models, features and extraction schemes,” Med Image Anal, 13(6), 819-45 (2009).
[10] F. M. hiri, L. Duong, C. Desrosiers *et al.*, "Vesselwalker: Coronary arteries segmentation using random walks and hessian-based vesselness filter." 918-921.
[11] C. Zhou, H. P. Chan, A. Chughtai *et al.*, “Automated coronary artery tree extraction in coronary CT angiography using a multiscale enhancement and dynamic balloon tracking (MSCAR-DBT) method,” Comput Med Imaging Graph, 36(1), 1-10 (2012).
[12] A. Kerkeni, A. Benabdallah, A. Manzanera *et al.*, “A coronary artery segmentation method based on multiscale analysis and region growing,” Computerized Medical Imaging and Graphics, 48, 49-61 (2016).
[13] Y. Tian, Y. Pan, F. Duan *et al.*, “Automated Segmentation of Coronary Arteries Based on Statistical Region Growing and Heuristic Decision Method,” Biomed Res Int, 2016, 3530251 (2016).
[14] G. Yang, P. Kitslaar, M. Frenay *et al.*, “Automatic centerline extraction of coronary arteries in coronary computed tomographic angiography,” Int J Cardiovasc Imaging, 28(4), 921-33 (2012).
[15] Y. Zheng, M. Loziczonek, B. Georgescu *et al.*, [Machine learning based vesselness measurement for coronary artery segmentation in cardiac CT volumes] SPIE, MI (2011).
[16] X. Dong, Y. Lei, T. Wang *et al.*, “Automatic multiorgan segmentation in thorax CT images using U-net-GAN,” Med Phys, 46(5), 2157-2168 (2019).
[17] Y. B. Fu, T. R. Mazur, X. Wu *et al.*, “A novel MRI segmentation method using CNN-based correction network for MRI-guided adaptive radiotherapy,” Medical Physics, 45(11), 5129-5137 (2018).
[18] Y. Lei, S. Tian, X. He *et al.*, “Ultrasound prostate segmentation based on multidirectional deeply supervised V-Net,” Med Phys, 46(7), 3194-3206 (2019).
[19] Y. Lei, T. Wang, S. Tian *et al.*, “Male pelvic multi-organ segmentation aided by CBCT-based synthetic MRI,” Phys Med Biol, (2019).
[20] J. Wu, J. Xin, X. Yang *et al.*, “Deep morphology aided diagnosis network for segmentation of carotid artery vessel wall and diagnosis of carotid atherosclerosis on black-blood vessel wall MRI,” Med Phys, 46(12), 5544-5561 (2019).
[21] X. Dong, Y. Lei, S. Tian *et al.*, “Synthetic MRI-aided multi-organ segmentation on male pelvic CT using cycle consistent deep attention network,” Radiother Oncol, 141, 192-199 (2019).
[22] B. Wang, Y. Lei, S. Tian *et al.*, “Deeply supervised 3D fully convolutional networks with group dilated convolution for automatic MRI prostate segmentation,” Med Phys, 46(4), 1707-1718 (2019).
[23] T. Wang, Y. Lei, G. Shafai-Erfani *et al.*, "Learning-based automatic segmentation on arteriovenous malformations from contract-enhanced CT images."
[24] Y. Lei, X. Dong, Z. Tian *et al.*, “CT prostate segmentation based on synthetic MRI-aided deep attention fully convolution network,” Medical Physics, doi:10.1002/mp.13933.
[25] Y. Lei, Y. Liu, X. Dong *et al.*, "Automatic multi-organ segmentation in thorax CT images using U-Net-GAN." 10950.
[26] Y. Lei, T. Wang, B. Wang *et al.*, "Ultrasound prostate segmentation based on 3D V-Net with deep supervision." 10955.

[27] B. Wang, Y. Lei, J. J. Jeong *et al.*, "Automatic MRI prostate segmentation using 3D deeply supervised FCN with concatenated atrous convolution." 10950.
[28] B. Wang, Y. Lei, T. Wang *et al.*, "Automated prostate segmentation of volumetric CT images using 3D deeply supervised dilated FCN." 10949.
[29] T. Wang, Y. Lei, H. Tang *et al.*, "A learning-based automatic segmentation method on left ventricle in SPECT imaging." 10953.
[30] T. Wang, Y. Lei, H. Tang *et al.*, "A learning-based automatic segmentation and quantification method on left ventricle in gated myocardial perfusion SPECT imaging: A feasibility study," Journal of Nuclear Cardiology, doi:10.1007/s12350-019-01594-2, (2019).
[31] T. Wang, Y. Lei, S. Tian *et al.*, "Learning-based automatic segmentation of arteriovenous malformations on contrast CT images in brain stereotactic radiosurgery," Medical Physics, 46(7), 3133-3141 (2019).
[32] W. Huang, L. Huang, Z. Lin *et al.*, "Coronary Artery Segmentation by Deep Learning Neural Networks on Computed Tomographic Coronary Angiographic Images." 608-611.
[33] J. M. Wolterink, R. W. van Hamersvelt, M. A. Viergever *et al.*, "Coronary artery centerline extraction in cardiac CT angiography using a CNN-based orientation classifier," Med Image Anal, 51, 46-60 (2019).
[34] J. M. Wolterink, T. Leiner, and I. Išgum, "Graph Convolutional Networks for Coronary Artery Segmentation in Cardiac CT Angiography."
[35] R. B. Girshick, "Fast R-CNN," 2015 IEEE International Conference on Computer Vision (ICCV), 1440-1448 (2015).
[36] K. He, G. Gkioxari, P. Dollár *et al.*, "Mask R-CNN," IEEE transactions on pattern analysis and machine intelligence, (2018).
[37] S. Ren, K. He, R. B. Girshick *et al.*, "Faster R-CNN: Towards Real-Time Object Detection with Region Proposal Networks," IEEE Transactions on Pattern Analysis and Machine Intelligence, 39, 1137-1149 (2015).
[38] X. Yang, N. Wu, G. Cheng *et al.*, "Automated segmentation of the parotid gland based on atlas registration and machine learning: a longitudinal MRI study in head-and-neck radiation therapy," International Journal of Radiation Oncology* Biology* Physics, 90(5), 1225-1233 (2014).
[39] J. Leipsic, S. Abbara, S. Achenbach *et al.*, "SCCT guidelines for the interpretation and reporting of coronary CT angiography: a report of the Society of Cardiovascular Computed Tomography Guidelines Committee," J Cardiovasc Comput Tomogr, 8(5), 342-58 (2014).
[40] C. A. Taylor, T. A. Fonte, and J. K. Min, "Computational fluid dynamics applied to cardiac computed tomography for noninvasive quantification of fractional flow reserve: scientific basis," J Am Coll Cardiol, 61(22), 2233-41 (2013).